Fluidization of Solids with CO_2 at Pressures from Ambient to Supercritical

Antonio Marzocchella and Piero Salatino
Dipt. di Ingegneria Chimica, Università di Napoli "Federico II," Istituto di Ricerche sulla Combustione–C.N.R., 80125 - Napoli, Italy

Beds of two granular materials belonging to groups A-B and B of the Geldart classification of powders were fluidized by carbon dioxide at 35°C and at 1 to 80 bar. Within this pressure interval, spanning from subcritical to supercritical conditions, the fluid density changes from the values typical of dilute gases to those of liquids. The hydrodynamic behavior of the bed changes accordingly. The bed behavior was investigated by visual inspection of the bed and by analysis of the time series of the pressure drop across the bed and of the heat-transfer coefficient between the bed and a hot wire probe. The boundaries between different captive fluidization regimes — incipient fluidization, onset of bubbling, and the incipient and fully established turbulent regime — were mapped in gas superficial velocity vs. fluid density phase planes for the two granular materials investigated.

Introduction

Increasing interest for fluidized-bed technology at high pressures has been only partly supported by better understanding hydrodynamic behavior of solids fluidized with dense gases. Knowlton (1992) and, more recently, Yates (1996) pointed out the established features and the open issues associated with the use of dense fluidized suspensions. The variety of captive fluidization regimes (homogeneous, bubbling-slugging, and turbulent) and the implication of bed hydrodynamics on the performance of fluidized-bed units call for more of an extensive characterization of the dependence of regime transitions on operating conditions (superficial velocity, fluid density and viscosity, and properties of bed solids).

Research in this field has been mostly focused on the assessment of conditions for the onset of the bubbling regime and to characterization of bubble properties and fluidization quality in pressurized fluidized beds (Knowlton, 1977; Varadi and Grace, 1978; Guedes de Carvalho et al., 1978; Subzwari et al., 1978; King and Harrison, 1980; Sobreiro and Monteiro, 1982; Rowe et al., 1982, 1983; Barreto et al., 1983; Chitester et al., 1984; Weimer and Quarderer, 1985; Hoffman and Yates, 1986; Jacob and Weimer, 1987; Chan et al., 1987; Hatano and Kido, 1992; Wiman and Almstedt, 1997, 1998). The debate is still open on the mechanistic aspects underlying the establishment of a homogeneously expanded state of the bed (Clift, 1993). Several articles have addressed the relative importance of hydrodynamic forces (Anderson and Jackson, 1968; Wallis, 1969; Verloop and Heertjes, 1970; Garg and Pritchett, 1975; Foscolo and Gibilaro, 1984; Batchelor, 1988) vs. interparticle forces (Baerns, 1966; Massimilla et al., 1972; Donsì and Massimilla, 1973; Rietema, 1973; Mutsers and Rietema, 1977; Rietema and Piepers, 1990; Tsinontides and Jackson, 1993) as the factors stabilizing the homogeneously expanded state of the bed. The dispute was partly reconciled by Martin (1983) who underlined the distinction between *particulate fluidization* (the homogeneous expansion is stabilized by hydrodynamics only) and *delayed bubbling* (interparticle forces promote homogeneous expansion over a limited range of bed voidages).

The establishment of turbulent fluidization under pressurized conditions has received comparatively little attention (Lanneau, 1960; Canada and McLaughlin, 1978; Yang and Chitester, 1988; Cai et al., 1989; Lancia et al., 1990; Tsukada et al., 1993). The mechanisms of bubble growth/splitting and the balance between visible bubble flow and interstitial flow affect the transition between aggregative and turbulent fluidization. The way operating pressure influences these phenomena deserves further investigation.

Correspondence concerning this article should be addressed to P. Salatino.

Table 1. Properties of the Fluid and of the Solids

Pressure II, bar	1	20	40	60	80
Temperature, °C	18	35	35	35	35
Fluid density, kg/m^3	1.8	36	85	150	480
Fluid viscosity, Pa·s	1.46×10^{-5}	1.65×10^{-5}	1.73×10^{-5}	1.91×10^{-5}	4.18×10^{-5}
Archimedes number,					
Ballotini 88 μm	143	2,100	4,420	6,300	4,930
Ballotini 175 μm	1,080	17,600	35,000	51,000	28,300

Crowther and Whitehead (1978), while interested in supercritical extraction of coal, pioneered the use of gases under nearly- or supercritical conditions as fluidizing media to investigate the behavior of pressurized fluidized beds. This direction was eventually followed by Salatino et al. (1991), Poletto et al. (1993) and, more recently, by Liu et al. (1996) and Marzocchella and Salatino (1996, 1998). All these studies took advantage of the property of nearly-critical fluids to undergo dramatic change of density upon a moderate change in pressure and/or temperature. At the same time, fluid viscosity changes to a much lesser extent and is generally closer to values typical of dilute gases. This feature enables the spanning of a broad range of fluidization patterns—from those typical of dilute gases to those typical of liquids—by changing the fluid pressure over a relatively limited range.

In this work, operation with nearly-critical carbon dioxide has the objective of investigating captive fluidization regime transitions over a broad range of gas densities with two solid materials. Several experimental techniques have been used to mark incipient fluidization, the onset of a bubbling regime, and the incipient and full transition to the turbulent regime. In particular, a novel technique based on the analysis of the time-series of the heat-transfer coefficient between the fluidized bed and a hot wire probe—already successful at atmospheric pressure (Boerefijn et al., 1996, 1999)—has been extended to operation under pressure. It has proven to be the most reliable method for marking the onset of bubbling under the relatively smooth fluidization conditions typical of pressurized fluidization. Boundaries of regions corresponding to the different fluidization regimes have been mapped in gas superficial velocity - fluid density phase planes.

Experimental Studies

Materials

Carbon dioxide at pressures ranging from 1 to 80 bar was used as a fluidizing medium. The critical pressure is 72.9 bar, and the critical temperature 31.1°C. A supercritical operating temperature of 35°C was used in all experiments, but in those experiments carried out at atmospheric pressure, the operating temperature was 18°C.

Glass beads used as bed materials had a density of 2,440 kg/m^3 and were sieved in either the 75–100 μm (Ballotini, 88 μm) or the 150–200 μm (Ballotini, 175 μm) size ranges. They, respectively, belong to the A-B and to the B groups of the Geldart classification of powders referred to the fluidization behavior at atmospheric pressure.

Table 1 shows the operating conditions of the experiments and the properties of CO_2, as well as the Archimedes number of the fluid-solid systems used in the experiments.

Experimental apparatus

The apparatus is shown in Figure 1. The fluidization column (30-mm-ID) consisted of a lower section (600-mm-high) made of a polycarbonate tube that enables visual inspection of the bed, and of a stainless steel upper section (700-mm-high) serving as a disengagement section. Carbon dioxide, at temperatures ranging from ambient to 80°C and pressures from ambient to 100 bar, can be continuously fed to the column via a recirculation loop embodying a diaphragm compressor (C), a back pressure regulating valve (K1), a water cooled heat exchanger (E1), and an electrical heater (E2). The maximum throughput in the loop was of about 100 kg/h. The CO_2 flow rate was measured by a Coriolis force-based mass flowmeter (EXAC, FI1), which also provided a measure of the fluid density. The pressure pulsation dampers (D1 and D2) were sized in order to reduce pressure fluctuations in

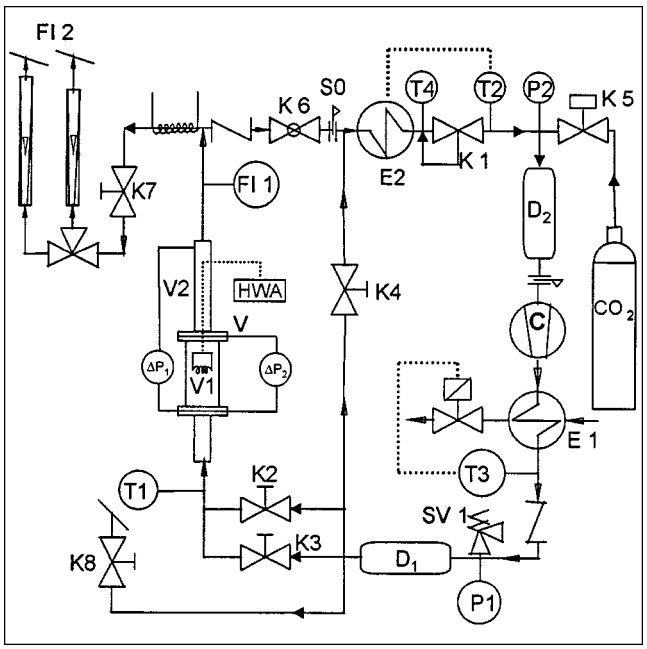

Figure 1. Experimental apparatus.

C compressor; D1, D2 pressure pulsation dampers; ΔP differential pressure transducer; HWA hot wire anemometer; E1 water-cooled heat exchanger; E2 electric heater; FI1 mass flowmeter and density meter; FI2 rotameters; K1 back-pressure regulating valve; K2, K3 flow regulation valves; K4 bypass regulation valve; K5, K6 on-off valves; K7 fine metering valve; K8 venting valve; P1, P2 operating pressure transducers; S0 filter; SV1 relief valve; T1, T3 platinum thermometers; T2, T4 thermocouples; V fluidization column; V1 polycarbonate section of the column; V2 stainless-steel disengagement section of the column.

the vessel. A filter (S0) downstream of the fluidization column collected any particles possibly entrained from the fluidized bed.

Two differential pressure transducers (Figure 1) measured the pressure drop over the bed ΔP_1 and over the first 30 cm of the fluidization column, respectively. Their upper bandwidth limit was about 100 Hz.

A hot wire anemometer (HWA), which operated in the constant temperature mode, provided the measure of the heat-transfer coefficient between the suspension and a thin platinum wire. Details on the operation of the anemometer at atmospheric pressure are given by Boerefijn et al. (1996, 1999). The hot wire probe was modified in order to be operated at pressures up to 100 bar. The hot wire was 20 mm long and 50 μm in diameter, and kept tight and horizontal by two brass branches at a constant level of about 190 mm above the distributor.

Signals from the differential pressure transducers and from the anemometer were simultaneously recorded by a chart recorder and logged at a sampling rate of 500 Hz on a personal computer equipped with an anti-aliasing card and a 16 bit A/D converter. The anti-aliasing card prevented the acquired signals from being affected by high frequency noise. The low-pass cut-off frequency was generally set at 30 Hz and did not interfere with oscillatory phenomena typical of a fluidized bed.

Experimental procedure

The fluidization column was charged with the bed solids up to a static bed height of about 240 mm, corresponding to 250 g of bed material. Air was then removed from the system by repeatedly pressurizing (up to around 3 bar) and de-pressurizing the plant with carbon dioxide. Finally, the plant was brought to the operating pressure. At the beginning of each experiment, the compressor was started, then fine adjustment of the operating pressure (by the valve K1) and temperature (by the temperature controller T3-E1) was accomplished. The steady state of the plant was typically established in less than one hour. During the experiments, the gas superficial velocity (U) was quasi-steadily increased from zero up to a maximum value that was limited by one of the following constraints:

- The maximum possible throughput in the loop (100 kg/h)
- The maximum expansion of the bed compatible with its visual inspection in the transparent section of the fluidization column (600 mm)
- The establishment of a gas superficial velocity larger than the transport velocity of the bed at the specified conditions. This occurrence was prevented by monitoring the pressure drop across the bed ΔP_1 that was never allowed to become appreciably lower than the buoyant weight per unit cross-sectional area of the bed.

The process pressure and temperature were continuously monitored during the operation. The fluid density considered in the data analysis was the one measured by the flow- and density-meter FI1 when it was higher than the lower sensitivity limit of the instrument (50 kg/m^3). Below this threshold, fluid density was calculated as a function of pressure and temperature by means of the real gases equation of state accounting for nonidealities through a compressibility factor. The viscosity of the fluid was calculated as indicated by Poletto et al. (1993).

Under each set of operating conditions, the behavior of the bed was characterized by the following techniques:

(1) Visual inspection of the bed, including continuous recording of bed height vs. fluid velocity. Results were determined in terms of the usual (log ϵ) vs. (log U) Richardson-Zaki (1954) plots, where ϵ is the bed voidage

(2) Time resolved recording of the pressure drop across the bed ΔP_1 at different U values

(3) Time resolved measurement of the heat-transfer coefficient h between the bed and the hot wire probe at different U values.

Both time-series were eventually worked out to yield statistical and spectral parameters. In particular, the average and the variance of the time-series were adopted in the present work to mark singularities associated with fluidization regime transitions.

Experimental Results

Assessment of incipient fluidization

Figures 2A and 2B report the pressure drop across the bed ΔP_1 as a function of the fluid superficial velocity U recorded in experiments carried out with 88 and 175 μm Ballotini at different absolute pressures. It can be noted that the bed pressure drop under fluidized conditions decreases as pressure increases. This is a consequence of the decreasing value of the density difference between particles and fluid ($\rho_s - \rho_f$) as operating pressure increases. Figures 3A and 3B report the bed voidage ϵ as a function of gas superficial velocity U measured in the same experiments. Incipient fluidization conditions were marked, as usual, as the intersections in Figures 2 and 3 between the curves relative to the fixed state and those relative to the fully fluidized state of the beds. Values of the minimum fluidization velocities are reported in Table 2 together with those estimated by means of the relationship proposed by Chitester et al. (1984).

Uniform bed expansion

Visual inspection of the bed suggested that the larger the fluid pressure, the broader the ranges of U within which homogeneous fluidization occurred for both solids. Bed voidage vs. gas superficial velocity in the homogeneous expansion range (Figure 3) were correlated according to the Richardson and Zaki (1954) equation $U = U_0 \epsilon^n$. Best fit parameters U_0 and n for each operating condition are reported in Table 2. Notably, U_0 and n were close to theoretical values of particles terminal velocity U_t (calculated according to Haider and Levenspiel, 1989) and of Richardson and Zaki (1954) exponents, respectively.

A reproducible, though limited, range of uniform expansion is observed at 1 bar fluid pressure with both materials. This behavior is expected in the case of 88 μm glass beads, lying at the boundary between groups A and B of the Geldart classification of powders. It is unexpected for Ballotini 175 μm belonging to the B group. This behavior might be explained by considering that experiments at 1 bar were carried out at a temperature lower than the critical temperature of

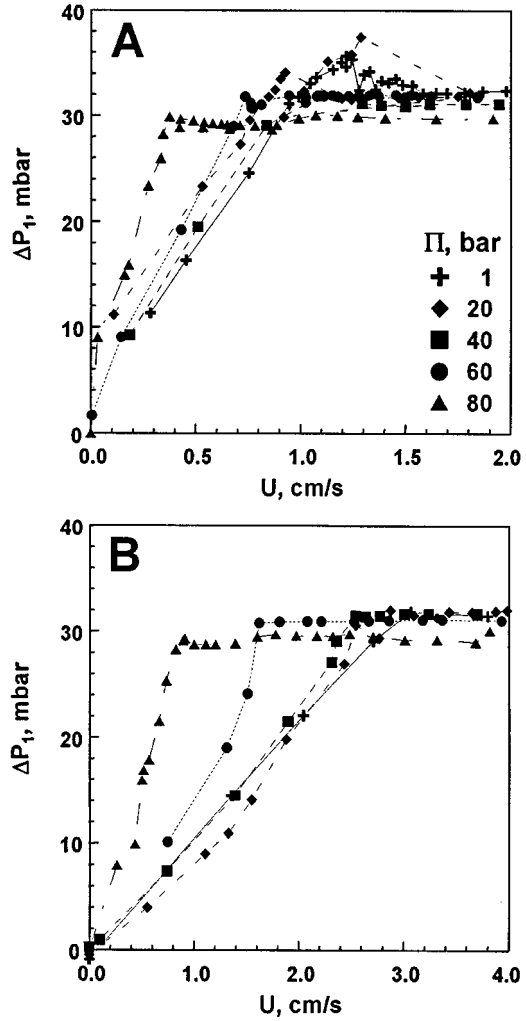

Figure 2. Pressure drop over the bed vs. superficial fluid velocity.

(A) 88 μm Ballotini; (B) 175 μm Ballotini.

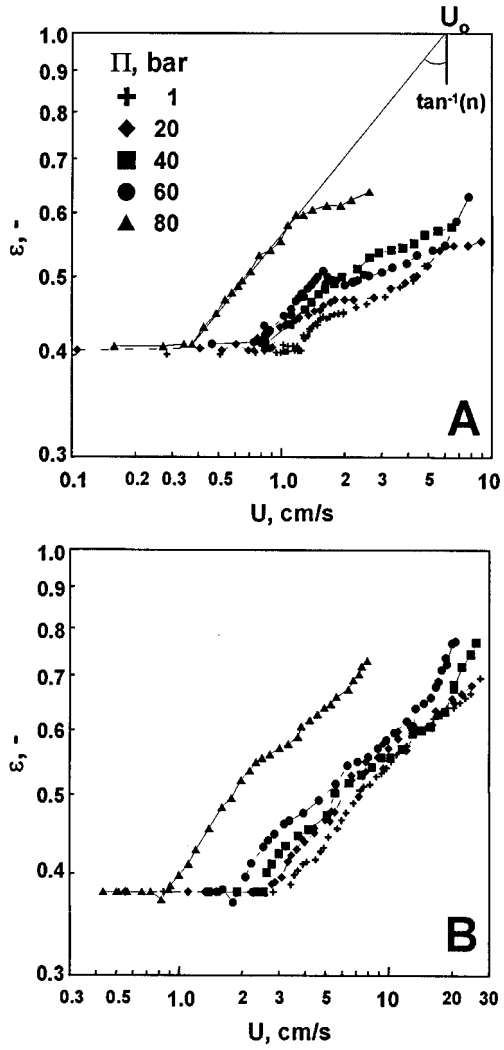

Figure 3. Average bed voidage vs. superficial fluid velocity.

(A) 88 μm Ballotini; (B) 175 μm Ballotini.

carbon dioxide. Capillary condensation of CO_2 and consequent particle bridging at the subcritical conditions of these tests might have been responsible for delayed bubbling (D'Amore et al., 1979).

Assessment of the onset of the bubbling regime

Marking the onset of bubbling by visual inspection of the bed has been always associated with some uncertainty in this

Table 2. Parameters of Bed Expansion and of Fluidization Regime Transitions

Material	Ballotini 88 μm					Ballotini 175 μm				
Π, bar	1	20	40	60	80	1	20	40	60	80
U_{mf}, cm/s*	1.1 (1.01)	0.86 (0.90)	0.90 (0.83)	0.74 (0.76)	0.30 (0.33)	3.0 (3.96)	2.7 (3.08)	2.5 (2.54)	1.8 (2.09)	0.82 (0.99)
U_{mb}, cm/s	1.5	1.2	1.4	1.6	1.1	3.65	3.32	3.1	3.0	1.6
ϵ_{mb},	0.44	0.44	0.47	0.50	0.58	0.40	0.41	0.43	0.45	0.50
U_c, cm/s	26.7	18	8.8	6.8	2.4	> 16	17	13	7.5	2.5
U_k, cm/s	30	> 23	13	11.5	3.2	> 16	> 25	20 .	13	2.7
U_0, cm/s	38	23	15	13	6.9	—	43	37	20	10
U_t, cm/s**	51	24	18	14	7	125	45	32	24	12
$n^\dagger$	3.9 (3.8)	3.6 (3.1)	3.1 (2.8)	3.1 (2.9)	3.0 (2.9)	—	2.6 (3.1)	3.1 (2.5)	2.5 (2.5)	2.7 (2.5)

*Value in parenthesis calculated according to Chitester et al. (1984).
**Calculated according to Haider and Levenspiel (1989).
†Value in parenthesis calculated according to Richardson and Zaki (1954).

and in previous investigations. This is especially true as pressure increases, since fluidization becomes smoother even under aggregative fluidization conditions.

An alternative method for the assessment of incipient bubbling conditions is represented by the analysis of plots in Figure 3. Departure from the linearity of (log ϵ) vs. (log U) plots could be interpreted as the bubbling onset. However, assessment of this transition from singularities in the (log ϵ) vs. (log U) plots is also associated with some uncertainty.

The most effective method for the assessment of mimimum bubbling conditions has proven to be the analysis of the time-series of the bed-wire heat-transfer coefficient. It has been suggested (Kumar et al., 1993; Boerefijn et al., 1996, 1999) that fluctuations of h are related to particle motion rather than to turbulence intrinsic to the fluid, even under dense bed fluidization conditions and regardless of how large is the contribution to h by fluid convection. Accordingly, the hot wire anemometer would be sensitive to particles fluctuations as small as those induced by the passage of a voidage wave, the bubble precursor.

Figure 4 reports typical time-series of the heat-transfer coefficient recorded with beds of the two solids at two pressure levels. Two gas superficial velocities have been considered for each system, one belonging to the uniform expansion range and the other corresponding to well established bubbling regime. For comparison, a similar time-series recorded in a bed of 175 μm glass beads fluidized by water is reported (Boerefijn et al., 1996). The different patterns associated with aggregative and homogeneous fluidization are easily recognized and will be further discussed in the following section.

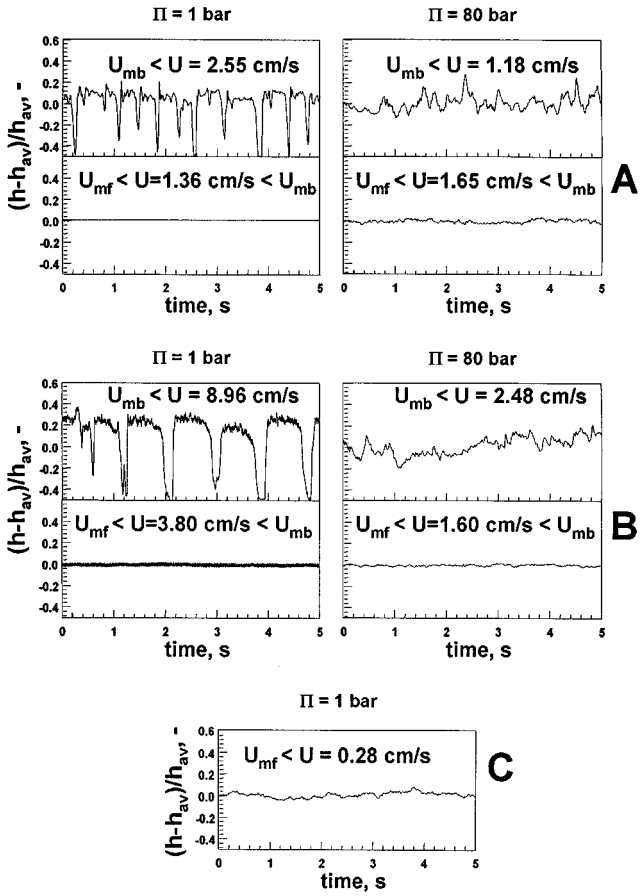

Figure 4. Time series of the dimensionless heat-transfer coefficient.

(A) CO_2-Ballotini 88 μm; (B) CO_2-Ballotini 175 μm; (C) water-Ballotini 175 μm.

Figure 5 reports the average heat-transfer coefficient h as a function of the gas superficial velocity. In the same figure, the variance σ_h^2 of the time-series of the anemometric signal is plotted. Plots are restricted to ranges of gas superficial velocities close to incipient fluidization and bubbling. h vs. U plots denote a discontinuity corresponding to the bubbling onset at the lowest pressures. On the contrary, h increases smoothly with U at high pressure without any remarkable singularity. The σ_h^2 vs. U plots display a singularity with a sudden change in the slope at a superficial velocity U corresponding to the bubbling onset (U_{mb}) at any operating pressure and with both bed solids. No such singularity is instead observed at the incipient fluidization, unless it is coincident with (or close to) the bubbling onset (this was the case for both solids at atmospheric pressure). It is concluded that σ_h^2 vs. U plots effectively reflect particle mobility associated with the bubbling onset. Values of U_{mb} determined according to this procedure are reported in Table 2 together with the bed voidage ϵ_{mb} at the incipient bubbling. Values of ϵ_{mb} closely agree with those obtained in a previous investigation (Poletto et al., 1993).

The method based on the analysis of the σ_h^2 vs. U plots is based on a concept similar to the one put forward by Taylor et al. (1974) and later developed by Hong et al. (1990) to identify the minimum fluidization velocity from analysis of the variance ($\sigma^2_{\Delta P_1}$) of the pressure drop across the bed. These authors related the sharp increase in $\sigma^2_{\Delta P_1}$ with U for Geldart group B particles to the solids oscillations at the bed surface due to bubbles bursting. Instead, for particles characterized by the existence of a uniform bed expansion, the sharp increase in $\sigma^2_{\Delta P_1}$ with U is rather related to the bubbling onset. The $\sigma^2_{\Delta P_1}$ vs. U analysis method was also used in this study. Figure 5 reports $\sigma^2_{\Delta P_1}$ vs. U plots in the vicinity of the incipient fluidization and incipient bubbling velocities. The onset of bubbling is marked by a singularity in the curves that, however, is much less pronounced than the one appearing in the corresponding σ_h^2 vs. U plots. When comparing the two methods, it should be noted that pressure fluctuations are related to an integral property of the bed, namely the periodic change in the bed height. Fluctuations of heat-transfer coefficient, on the other hand, are related to the local perturbations induced by the passage of bubbles. The local character of the σ_h^2 vs. U plot, as opposed to the integral character of $\sigma^2_{\Delta P_1}$ vs. U plots, might explain the better accuracy of the U_{mb} assessment based on the former analysis. Agreement between the incipient bubbling velocities evaluated with the two techniques is in any case satisfactory.

It must be noted that, because of the relatively small column diameter, slugging fluidization is established at large fluidization velocities and at low pressures, while bubbling is established at any superficial velocity beyond U_{mb} and at high (> 20 bar) pressures.

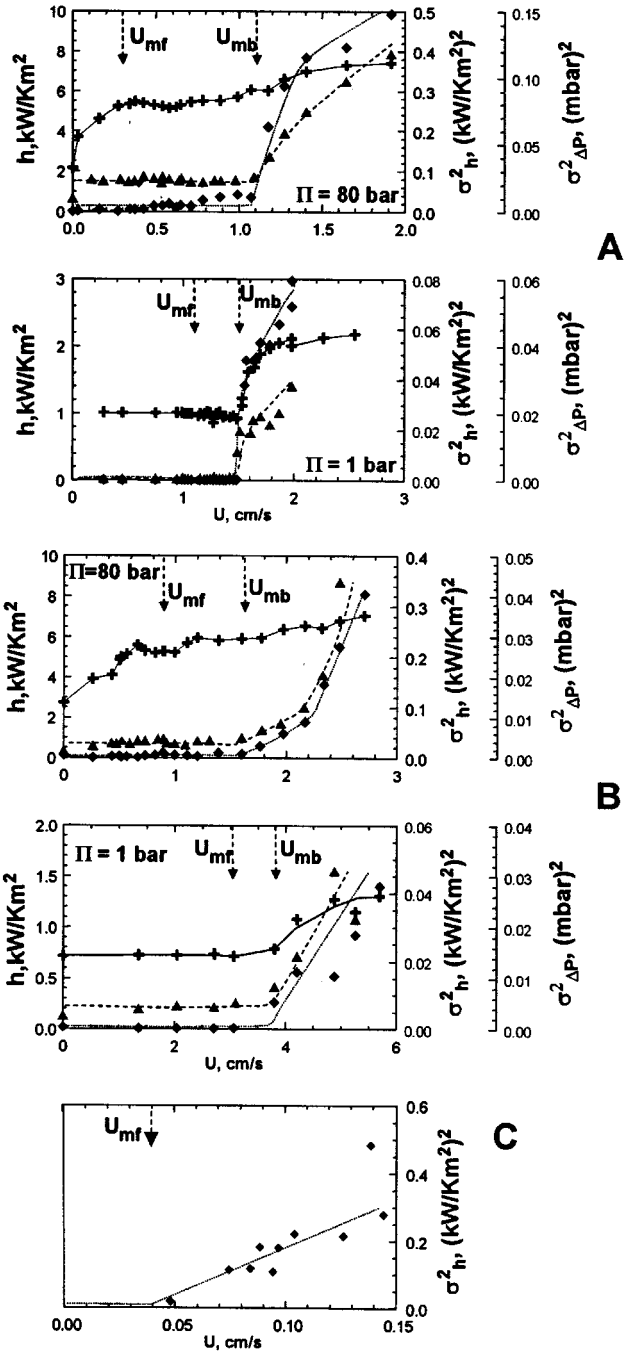

Figure 5. Heat-transfer coefficient (+), its variance (♦) and pressure drop variance (▲) as functions of fluid superficial velocity in the vicinity of incipient fluidization and bubbling.

(A) CO_2-Ballotini 88 μm; (B) CO_2-Ballotini 175 μm; (C) water-Ballotini 175 μm.

Assessment of the transition to the turbulent regime

Figure 6 shows the dimensionless variance of the pressure drop across the bed ($\sigma^2_{\Delta P_1}/\Delta P_1^2$) as a function of the gas superficial velocity at different operating pressures for the 88 μm and 175 μm glass beads. The $\sigma^2_{\Delta P_1}/\Delta P_1^2$ vs. U pattern is the well-known bell-shaped curve (Yerushalmi and Avidan, 1985). Gas superficial velocities at which $\sigma^2_{\Delta P_1}/\Delta P_1^2$ is at a maximum and at which it levels off, have been assumed, respectively, as the beginning U_c and the end U_k of the transition to the turbulent fluidization regime (Yerushalmi and Avidan, 1985). Note that no detectable decrease in the pressure drop across the bed was observed over several minutes of operation of the bed even at fluid superficial velocities over U_k. Furthermore, the original bed height was always reobtained upon defluidization at the end of the experiments. These observations, together with the absence of solids in the filter S0 (Figure 1), suggested that elutriation was not significant under the experimental conditions tested. Therefore, leveling off of the $\sigma^2_{\Delta P_1}/\Delta P_1^2$ could not be attributed to bed entrainment (Geldart and Rhodes, 1986).

Note in Figure 6 that the amplitude of pressure fluctuations first increases, then decreases with the operating pressure at a given fluid superficial velocity U. This effect might be related to the non-monotonic pressure-dependence of the maximum stable bubble size observed by other authors (such as Hoffmann and Yates, 1986; Olowson and Almstedt, 1990; Cai et al., 1994). It is observed that the $\sigma^2_{\Delta P_1}/\Delta P_1^2$ becomes very small and is significantly affected by the experimental error beyond 60 bar, consistently with the observation that fluidization at high pressure is smooth even under aggregative fluidization conditions.

Discussion

Results of the evaluation of fluidization regime transitions are summarized in Figures 7A and 7B for 88 μm and 175

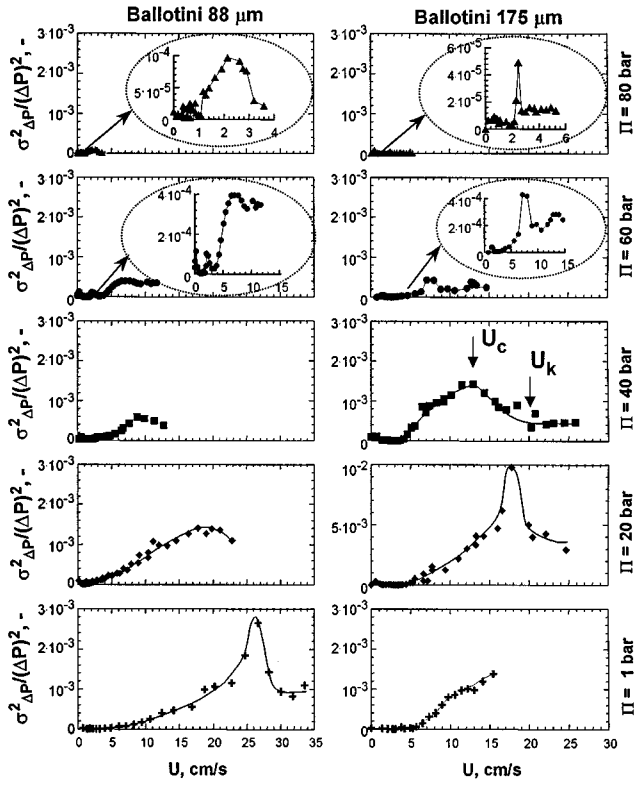

Figure 6. Dimensionless variance of the bed pressure drop vs. superficial fluid velocity.

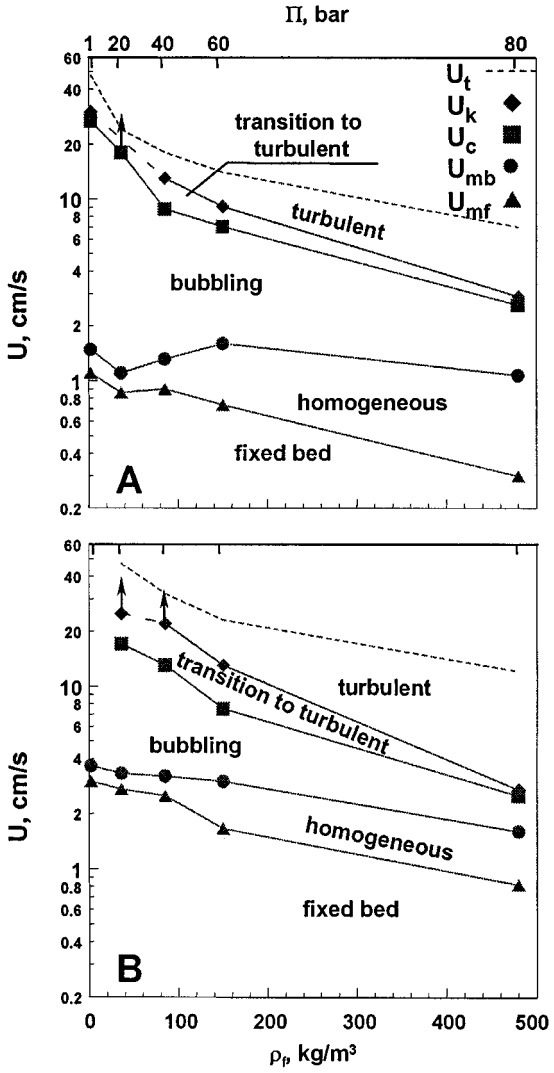

Figure 7. Velocities at regime transitions vs. fluid density.

(A) Ballotini 88 μm; (B) Ballotini 175 μm.

μm glass beads, respectively. These figures show data points corresponding to regime transitions in a gas superficial velocity vs. fluid density phase plane. The theoretical value of the particle terminal velocity (according to Haider and Levenspiel, 1989) is also reported.

The figures summarize the main features of the fluidization under pressure of the two materials.

Incipient Fluidization. Gas superficial velocity at incipient fluidization decreases as the fluid density increases. This effect is enhanced as the operating pressure is above 60 bar.

Homogeneous Expansion and Onset of Bubbling Regime. The region of homogeneous fluidization is wider for the finest solids and broadens as the fluid density increases. For the finest particles, a nonmonotonic trend of U_{mb} vs. fluid density is observed, consistently with observations of Chitester et al. (1984).

The question is open as to whether homogeneous expansion of the bed observed under the conditions of the present work corresponds to *particulate fluidization* or rather to *delayed bubbling* regimes. According to the definitions given by Martin (1983), *particulate fluidization* is a state of the bed characterized by uniform concentration of relatively freely-moving particles with transient particle-particle contacts. The *delayed bubbling* is a state of the bed characterized by the formation of coherent skeletons of particles stabilized by interparticle forces. The cellular structure of the bed under the action of forces at the particle-particle contact points in homogeneously fluidized gas-solid systems was well documented by Massimilla et al. (1972) and Donsì and Massimilla (1973). Whether particulate fluidization or delayed bubbling regimes applies, not only is it relevant to the assessment of the mechanisms responsible for the stabilization of the uniformly expanded bed state, but it is also relevant to important properties of the fluidized suspension such as the extent and patterns of solids mixing and heat transfer.

Poletto et al. (1993) carried out an investigation on the nearly-critical fluidization of a broad range of solid materials. They suggested, on the basis of arguments concerning similarity, that criteria based on hydrodynamics alone could not explain the stabilization of the uniform bed expansion observed under the experimental conditions tested. This finding supported the view that a *delayed bubbling state* of the bed could have been stabilized by interparticle forces. Results obtained with the analysis of the time-series of the hot wire-bed heat-transfer coefficient apparently provide additional support to this view. Data in Figure 5 indicate that the variance of the heat-transfer coefficient is as negligible in the homogeneous fluidization regime as in the fixed-bed regime. On the contrary, values of σ_h^2 change abruptly upon increasing gas superficial velocity beyond U_{mb}. If fluctuations of h are associated to particles packets motion, as suggested by Boerefijn et al. (1996, 1999), the very low σ_h^2 implies that particle mobility is substantially hindered at gas superficial velocities comprised between incipient fluidization and incipient bubbling; hence, a delayed bubbling state is established. In agreement with this scenario is the comparison between the time-series of h—and its variance—recorded for the glass beads-CO_2 systems, within the homogeneous fluidization range, and those recorded in a truly particulate system, namely, 175 μm glass beads fluidized by water (Figures 4 and 5). Much broader oscillations, possibly related to larger particle mobility, are observed in the liquid-fluidized than in the homogeneously gas-fluidized beds. Correspondingly, the variance of h departs from zero at $U > U_{mf}$ in the liquid-fluidized bed (Figure 5C), whereas it departs from zero at $U > U_{mb}$ for the homogeneously gas-fluidized bed (Figures 5A and 5B).

Turbulent Fluidization. Transition to turbulent fluidization occurs at gas superficial velocities decreasing when pressure, hence fluid density increases. The velocity range of turbulent fluidization broadens mostly at the expense of the aggregative fluidization range. At the same time, the distinction between aggregative and turbulent fluidization regimes becomes less pronounced. Also, the U_c-U_k range narrows as pressure increases. Pressure is likely to affect this transition in a twofold way. On the one hand, average bubble size decreases as pressure increases, ultimately approaching the length scale of particles clusters. On the other hand, solid concentrations in the emulsion and in the lean phases of the

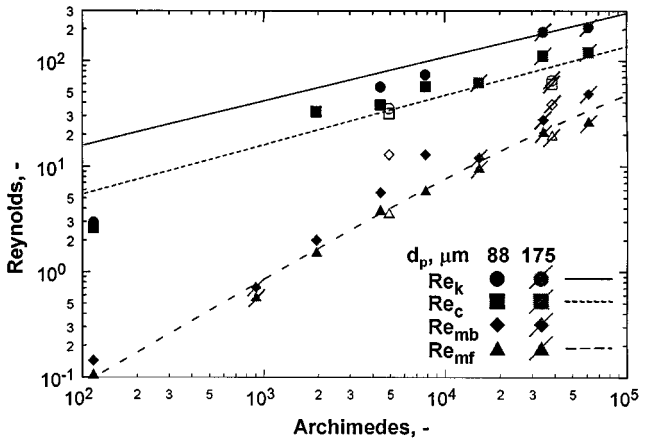

Figure 8. Map of fluidization regimes in terms of Reynolds vs. Archimedes numbers plots.

Lines represent literature correlations: Re_{mf} (Chitester et al., 1984); Re_c (Nakajima et al., 1991); Re_k (Bi and Fan, 1992).

bed in the bubbling state approach each other as pressure increases, as observed by Lanneau (1960). This is related to larger interstitial flow (and, conversely, smaller visible bubble flow) established with finer solids. Gilbertson et al. (1998) observed that bed voidage in bubbles departs significantly from unity as pressure increases. Lean phase ''densification'' and increasing expansion of the emulsion phase would then concur in making the transition between the bubbling and the turbulent regimes less sharp as pressure increases.

In the present study, U_c decreases as fluid pressure increases. The same trend was reported by Cai et al. (1989) and Tsukada et al. (1993), whereas Lancia et al. (1990) reported that U_c was barely affected by gas pressure. U_k decreases as pressure increases in agreement with findings of previous investigators (Yang and Chitester, 1984; Cai et al., 1989; Tsukada et al., 1993; Lancia et al., 1990).

Captive fluidization regimes have been replotted in dimensionless form in Figure 8 by reporting the particle Reynolds number at the regime transition velocity as a function of the Archimedes number of the fluid-solids system. In the same figure, correlations for the evaluation of U_{mf} (Chitester et al., 1984: $Re_{mf} = \sqrt{(28.7)^2 + 0.0494\,Ar} - 28.7$), U_c (Nakajima et al., 1991: $Re_c = 0.663\ Ar^{0.467}$), and U_k (Bi and Fan, 1992: $Re_k = 0.601\ Ar^{0.695}$ for $Ar \le 125$; $Re_k = 2.28\ \mathrm{Ar}^{0.419}$ for $Ar > 125$) are plotted for comparison. Note that only the first correlation was intended for use under pressurized conditions, with the others relying on experiments carried out at atmospheric pressure only. When looking at data points in Figure 8, it should be considered that the Archimedes number changes nonmonotonically as fluid pressure is increased, being maximum at $\Pi = 60$ bar.

The analysis of Figure 8 suggests that Re_{mf} calculated according to Chitester et al. (1984) agrees fairly well with the experimental data points estimated in the present study for the fine particles. It is slightly overestimated for the coarse material throughout the pressure range investigated. Reynolds numbers Re_{mb} estimated at the bubbling onset increase with the Archimedes number. Re_{mb} vs. Ar profiles for the two bed solids do not overlap with each other. Reynolds numbers Re_c at the incipient turbulent regime appear to be underestimated by an almost constant factor by the Nakajima et al. (1991) correlation. Reynolds numbers corresponding to the full establishment of the turbulent regime Re_k are poorly reproduced by the Bi and Fan (1992) correlations. These relationships suggest that, in the range of Archimedes numbers investigated, the velocity at the fully established turbulent regime U_k coincides with the transport velocity. This is in contrast to the results of the present study that indicate that a well developed turbulent regime may be established at superficial velocities above U_k at pressures higher than 20 bar.

Conclusions

The transition between captive fluidization regimes was investigated in experiments in which carbon dioxide at pressures ranging from subcritical to supercritical was used as fluidizing medium. The behavior of the fluidized suspension was characterized by visual inspection of the bed and statistical analysis of the time-series of the pressure drop across the bed, and of the heat-transfer coefficient between the fluidized suspension and the hot-wire probe.

Maps of fluidization regimes in a gas superficial velocity vs. fluid density phase plane were outlined for the two materials investigated. The following general features were observed:

- Incipient fluidization occurs at fluid superficial velocities that decrease as pressure, hence fluid density, increases, particularly beyond 60 bar
- Region of homogeneous fluidization broadens as the fluid density is increased
- Region of homogeneous fluidization is broader for the fine bed solids
- Statistical analysis of the heat-transfer coefficient fluctuations suggests that solids mobility is substantially hindered at gas superficial velocities within the range of uniform expansion
- Transition to turbulent fluidization occurs at decreasing fluid superficial velocities as pressure increases. The region in the gas velocity vs. the fluid density phase plane, within which turbulent fluidization is established, broadens as pressure increases, mostly at the expense of the aggregative fluidization region
- Fluidization becomes smoother even under aggregative fluidization conditions as fluid density increases. Correspondingly, the distinction between aggregative and turbulent fluidization becomes less pronounced.

Notation

Ar = Archimedes number $d_p^3\{[\rho_f(\rho_s - \rho_f)g]/\mu_f^2\}$
d_p = particle diameter, m
g = acceleration due to gravity, m/s^2
h = heat-transfer coefficient, kW/K·m^2
n = Richardson and Zaki exponent
ΔP_1 = bed pressure drop, mbar
U = fluid velocity, m/s
μ_f = fluid viscosity, Pa·s
ρ_f = fluid density, kg/m^3
ρ_s = particle density, kg/m^3
Π = operating pressure, bar
σ_h^2 = variance of h fluctuations, (kW/K·m^2)^2
$\sigma_{\Delta P_1}^2$ = variance of pressure drop fluctuations, mbar^2

Subscripts

av = average
c = beginning of transition to turbulent regime
k = end of transition to turbulent regime
mf = incipient fluidization
mb = incipient bubbling
t = particle terminal velocity

Literature Cited

Anderson, T. B., and R. Jackson, "A Fluid Mechanical Description of Fluidized Beds. Stability of the State of Uniform Fluidization," *Ind. Eng. Chem. Fundam.*, **7**, 12 (1968).

Baerns, M., "Effect of Interparticle Adhesive Forces on Fluidization of Fine Particles," *Ind. Eng. Chem. Fundam.*, **5**, 508 (1966).

Barreto, G. F., J. G. Yates, and P. N. Rowe, "The Effect of Pressure on the Flow of Gas in Fluidized Beds of Fine Particles," *Chem. Eng. Sci.*, **38**, 1935 (1983).

Batchelor, G. K., "A New Theory of the Instability of a Uniform Fluidized Bed," *J. Fluid Mech.*, **193**, 75 (1988).

Bi, H. T, and L.-S. Fan, "Existence of Turbulent Regime in Gas-Solid Fluidization," *AIChE J.*, **38**, 297 (1992).

Boerefijn, R., M. Poletto, and P. Salatino, "A Study of the Dynamic Behaviour of Fluidized Beds Based on a Hot Wire Anemometry Technique," *Fluidization VIII*, C. Laguerie and J. F. Large, eds., Engineering Foundation, New York, p. 51 (1996).

Boerefijn, R., M. Poletto, and P. Salatino, "Analysis of the Dynamics of Heat Transfer between a Hot Wire Probe and Gas Fluidized Beds," *Powder Technol.*, **102**, 53 (1999).

Cai, P., M. Schiavetti, G. De Michele, G. C. Grazzini, and M. Miccio, "Quantitative Estimation of Bubble Size in PFBC," *Powder Technol.*, **80**, 99 (1994).

Canada, G. S., and M. H. McLaughlin, "Large Particle Fluidization and Heat Transfer at High Pressures," *AIChE Symp. Ser.*, **74**, 27 (1978).

Chan, I. H., C. Shistla, and T. M. Knowlton, "The Effect of Pressure on Bubble Parameters in Gas Fluidized Beds," *Powder Technol.*, **53**, 217 (1987).

Clift, R., "An Occamist Review of Fluidized Bed Modelling," *AIChE Symp. Ser.*, **89**(296), 1 (1993).

Chitester, D. C., R. M. Kornosky, L.-S. Fan, and J. P. Danko, "Characteristics of Fluidization at High Pressure," *Chem. Eng. Sci.*, **39**, 253 (1984).

Crowther, M. E., and J. C. Whitehead, "Fluidization of Fine Particles at Elevated Pressure," *Fluidization*, J. F. Davidson and D. L. Keairns, eds., Cambridge University Press, p. 65 (1978).

D'Amore, M., G. Donsì, and L. Massimilla, "The Influence of Bed Moisture of Fluidization Characteristic of Fine Powders," *Powder Technol.*, **23**, 243 (1979).

Donsì, G., and L. Massimilla, "Bubble-Free Expansion of Gas Fluidized Beds of Fine Particles," *AIChE J.*, **19**, 1104 (1973).

Foscolo, P. U., and L. G. Gibilaro, "A Fully Predictive Criterion for the Transition Between Particulate and Aggregative Fluidization," *Chem. Eng. Sci.*, **39**, 1667 (1984).

Garg, S. K., and J. W. Pritchett, "Dynamics of Gas-Fluidized Beds," *J. Appl. Phys.*, **46**, 4493 (1975).

Geldart, D., and M. J. Rhodes, "From Minimum Fluidization to Pneumatic Transport—A Critical Review of the Hydrodynamics," *Circulating Fluidized Bed Technology I*, P. Basu, ed., Pergamon Press, Oxford, p. 21 (1986).

Gilbertson, M. A., D. J. Cheesman, and J. G. Yates, "Observations and Measurements of Isolated Bubbles in a Pressurised Gas-Fluidized Bed," *Fluidization IX*, L. S. Fan and T. M. Knowlton, eds., Engineering Foundation, New York, p. 61 (1998).

Guedes de Carvalho, J. R. F., D. F. King, and D. Harrison, "Fluidization of Fine Particles Under Pressure," *Fluidization*, J. F. Davidson and D. L. Keairns, eds., Cambridge University Press, Cambridge, U.K., p. 59 (1978).

Haider, A., and O. Levenspiel, "Drag Coefficient and Terminal Velocity of Spherical and Nonspherical Particles," *Powder Technol.*, **58**, 63 (1989).

Hatano, H., and N. Kido, "Bubble and Particle Behavior in a Pressurized Fluidized Bed," *Fluidization VII*, O. E. Potter and D. J. Nicklin, eds., Engineering Foundation, New York, p. 131 (1992)

Hoffmann, A. C., and J. G. Yates, "Experimental Observation of Fluidized Beds at Elevated Pressures," *Chem. Eng. Commun.*, **41**, 133 (1986).

Hong, S. C., B. R. Jo, D. S. Doh, and C. S. Choi, "Determination of Minimum Fluidization Velocity by the Statistical Analysis of Pressure Fluctuations in a Gas-Solid Fluidized Bed," *Powder Technol.*, **60**, 215 (1990).

Jacob, K. V., and A. W. Weimer, "High Pressure Particulate Expansion and Minimum Bubbling of Fine Carbon Powders," *AIChE J.*, **33**, 1698 (1987).

King, D. F., and D. Harrison, "The Bubble Phase in High Pressure Fluidized Beds," *Fluidization*, J. R. Grace and J. M. Matsen, eds., Plenum, New York, p. 101 (1980).

Knowlton, T. M., "High Pressure Fluidization Characteristics of Several Particulate Solids: Primarily Coal and Coal-Derived Materials," *AIChE Symp. Ser.*, **73** , 22 (1977).

Knowlton, T. M., "Pressure and Temperature Effects in Fluid-Particle Systems," *Fluidization VII*, O. E. Potter and D. J. Nicklin, eds., Engineering Foundation, New York, p. 27 (1992).

Kumar, S., K. Kusakabe, and L.-S. Fan, "Heat Transfer in Three-Phase Fluidized Beds Containing Low-density Particles," *Chem. Eng. Sci.*, **48**, 2407 (1993).

Lancia, A., R. Nigro, L. Santoro, and G. Volpicelli, "Effect of Pressure on the Transition From Slugging to Turbulent Flow Regimes of Fluidized Beds," *Chem. Biochem. Eng. Q.*, **4**, 205 (1990).

Lanneau, K. P., "Gas-Solids Contacting in Fluidized Beds," *Trans. Inst. Chem. Eng.*, **38**, 125 (1960).

Liu, D., M. Kwauk, and H. Li, "Aggregative and Particulate Fluidization—The Two Extremes of a Continuous Spectrum," *Chem. Eng. Sci.*, **51**, 4045 (1996).

Martin, P. D., "On the 'Particulate' and 'Delayed Bubbling' Regimes in Fluidisation," *Chem. Eng. Res. Des.*, **61**, 318 (1983).

Marzocchella, A., and P. Salatino, "The Dynamics of Fluidized Beds Under Pressure," *AIChE Symp. Series*, **92**(313), 25 (1996).

Marzocchella, A., and P. Salatino, "Pressure Effects on the Dynamics of Fluidized Beds," *World Congress on Particle Technology 3*, Brighton, U.K., paper n. 204, IChemE, U.K. (1998).

Massimilla, L., G. Donsì, and C. Zucchini, "The Structure of Bubble-Free Gas Fluidized Beds of Fine Fluid Cracking Catalyst Particles," *Chem. Eng. Sci.*, **27**, 2005 (1972).

Mutsers, S. M. P., and K. Rietema, "The Effect of Inter-Particle Forces on the Expansion of a Homogeneous Gas Fluidized Bed," *Powder Technol.*, **18**, 239 (1977).

Nakajima, M., M. Harada, M. Asai, R. Yamazaki, and G. Jimbo, "Bubble Fraction and Voidage in an Emulsion Phase in the Transition to a Turbulent Fluidized Bed," *Circulating Fluidized Bed Technology III*, P. Basu, M. Horio and M. Hasatani, eds., Pergamon Press, p. 71 (1991).

Olowson, P. A., and A. E. Almstedt, "Influence of Pressure and Fluidization Velocity on the Bubble Behaviour and Gas Flow Distribution in a Fluidized Bed," *Chem. Eng. Sci.*, **45**, 1733 (1990).

Poletto, M., P. Salatino, and L. Massimilla, "Fluidization of Solids with CO_2 at Pressures and Temperatures Ranging from Ambient to Nearly Critical Conditions," *Chem. Eng. Sci.*, **48**, 617 (1993).

Richardson, J. F., and W. T. Zaki, "Sedimentation and Fluidisation. Part I," *Trans. Instn. Chem. Engnrs*, **32**, 35 (1954).

Rietema, K., "The Effect of Interparticle Forces on the Expansion of a Homogeneous Gas-Fluidized Bed," *Chem. Eng. Sci.*, **28**, 1493 (1973).

Rietema, K., and H. W. Piepers, "The Effect of Interparticle Forces on the Stability of Gas-Fluidized Beds—I. Experimental Evidence," *Chem. Eng. Sci.*, **45**, 1627 (1990).

Rowe, P. N., P. U. Foscolo, A. C. Hoffmann, and J. G. Yates, "Fine Powders Fluidized at Low Velocity at Pressures up to 20 bar with Gases of Different Viscosity," *Chem. Eng. Sci.*, **37**, 1115 (1982).

Rowe, P. N., P. U. Foscolo, A. C. Hoffmann, and J. G. Yates, "X-ray Observation of Gas Fluidized Beds under Pressure," *Fluidization*, D. Kunii and R. Toei, eds., Engineering Foundation, New York, p. 53 (1983).

Salatino, P., M. Poletto, and L. Massimilla, "Stability of Uniform Gas Fluidized Beds Operated with CO_2 in Ranges of Pressure and

Temperature Between Ambient and Nearly-Critical Conditions,'' *IUTAM Symposium on Mechanics of Fluidized Beds*, Stanford University, CA (July 1–4, 1991).
Sobreiro, L. E. C., and J. L. F. Monteiro, ''The Effect of Pressure on Fluidized Bed Behaviour,'' *Powder Technol.*, **33**, 95 (1982).
Subzwari, M. P., R. Clift, and D. L. Pyle, ''Bubbling Behaviour of Fluidized Beds at Elevated Pressures,'' *Fluidization*, J. F. Davidson and D. L. Keairns, eds., Cambridge University Press, Cambridge, U.K., p. 50 (1978).
Taylor, P. A., M. H. Lorenz, and M. R. Sweet, ''Spectral Analysis of Pressure Noise in a Fluidized Bed,'' *Fluidization and its Applications*, H. Angelino, J. P. Couderc, H. Gibert, and C. Laguerie, eds., Cepadues-Editions, Toulouse, France, p. 90 (1974).
Tsinontides, S. C., and R. Jackson, ''The Mechanics of Gas Fluidized Beds with an Interval of Stable Fluidization,'' *J. Fluid Mech.*, **255**, 237 (1993).
Tsukada, M., D. Nakanishi, and M. Horio, ''The Effect of Pressure on Phase Transition from Bubbling to Turbulent Fluidization,'' *Int. J. Multiphase Flow*, **19**, 27 (1993).
Varadi, T., and J. R. Grace, ''High Pressure Fluidization in a Two-Dimensional Bed,'' *Fluidization*, J. F. Davidson and D. L. Keairns, eds., Cambridge University Press, Cambridge, U.K., p. 55 (1978).
Verloop, J., and P. M. Heertjes, ''Shock Waves as a Criterion for the Transition from Homogeneous to Heterogeneous Fluidization,'' *Chem. Eng. Sci.*, **25**, 825 (1970).
Wallis, G., *One-Dimensional Two-Phase Flow*, McGraw Hill, New York (1969).
Weimer, A. W., and G. J. Quarderer, ''On Dense Phase Voidage and Bubble Size in High Pressure Fluidized Beds of Fine Powders,'' *AIChE J.*, **31**, 1019 (1985).
Wiman, J., and A. E. Almstedt, ''Hydrodynamics, Erosion and Heat Transfer in a Pressurized Fluidized Bed: Influence of Pressure, Fluidization Velocity, Particle Size and Tube Bank Geometry,'' *Chem. Eng. Sci.*, **52**, 2677 (1997).
Wiman, J., and A. E. Almstedt, ''Influence of Pressure, Fluidization Velocity and Particle Size on the Hydrodynamics of a Freely Bubbling Fluidized Bed,'' *Chem. Eng. Sci.*, **53**, 2167 (1998).
Yang, W. C., and D. C. Chitester, ''Transition Between Bubbling and Turbulent Fluidization at Elevated Pressure,'' *AIChE Symp. Ser.*, **84**, 10 (1984).
Yates, J. G., ''Effects of Temperature and Pressure on Gas-Solid Fluidization,'' *Chem. Eng. Sci.*, **51**, 167 (1996).
Yerushalmi, J., and A. Avidan, ''High-Velocity Fluidization,'' *Fluidization*, 2nd ed., J. F. Davidson, R. Clift, and D. Harrison, eds., Academic Press, London, p. 225 (1985).

Manuscript received Apr. 5, 1999, and revision received Oct. 14, 1999.